ISSN 1674-1056
http://cpb.iphy.ac.cn
http://iopscience.iop.org/cpb
中国物理 B
Chinese Physics
中国物理 Chinese Physics B

Tunable coupling between Xmon qubit and coplanar waveguide resonator

He-Kang Li(李贺康), Ke-Min Li(李科敏), Hang Dong(董航), Qiu-Jiang Guo(郭秋江), Wu-Xin Liu(刘武新), Zhan Wang(王战), Hao-Hua Wang(王浩华), Dong-Ning Zheng(郑东宁)

Citation: Chin. Phys. B . 2019, 28(8): 080305. **doi:** 10.1088/1674-1056/28/8/080305
Journal homepage: http://cpb.iphy.ac.cn; http://iopscience.iop.org/cpb

What follows is a list of articles you may be interested in

Realization of *t*-bit semiclassical quantum Fourier transform on IBM's quantum cloud computer

Xiang-Qun Fu(付向群), Wan-Su Bao(鲍皖苏), He-Liang Huang(黄合良), Tan Li(李坦), Jian-Hong Shi(史建红), Xiang Wang(汪翔), Shuo Zhang(张硕), Feng-Guang Li(李风光)

Chin. Phys. B . 2019, 28(2): 020302. **doi:** 10.1088/1674-1056/28/2/020302

MatCloud, a high-throughput computational materials infrastructure: Present, future visions, and challenges

Xiaoyu Yang(杨小渝), Zongguo Wang(王宗国), Xushan Zhao(赵旭山), Jianlong Song(宋健龙), Chao Yu(虞超), Jiaxin Zhou(周嘉欣), Kai Li(李凯)

Chin. Phys. B . 2018, 27(11): 110301. **doi:** 10.1088/1674-1056/27/11/110301

Fabrication of Al air-bridge on coplanar waveguide

Zhen-Chuan Jin(金震川), Hai-Teng Wu(吴海腾), Hai-Feng Yu(于海峰), Yang Yu(于扬)

Chin. Phys. B . 2018, 27(10): 100310. **doi:** 10.1088/1674-1056/27/10/100310

Spin manipulation in semiconductor quantum dots qubit

Ke Wang(王柯), Hai-Ou Li(李海欧), Ming Xiao(肖明), Gang Cao(曹刚), Guo-Ping Guo(郭国平)

Chin. Phys. B . 2018, 27(9): 090308. **doi:** 10.1088/1674-1056/27/9/090308

Solid-state quantum computation station

Fanming Qu(屈凡明), Zhongqing Ji(姬忠庆), Ye Tian(田野), Shiping Zhao(赵士平)

Chin. Phys. B . 2018, 27(7): 070301. **doi:** 10.1088/1674-1056/27/7/070301

Tunable coupling between Xmon qubit and coplanar waveguide resonator*

He-Kang Li(李贺康)[1,3], Ke-Min Li(李科敏)[2], Hang Dong(董航)[2], Qiu-Jiang Guo(郭秋江)[2], Wu-Xin Liu(刘武新)[2], Zhan Wang(王战)[1,3], Hao-Hua Wang(王浩华)[2,†], and Dong-Ning Zheng(郑东宁)[1,3,4,‡]

[1] *Institute of Physics, Chinese Academy of Sciences (CAS), Beijing* 100190, *China*
[2] *Zhejiang Province Key Laboratory of Quantum Technology and Device, Department of Physics, Zhejiang University, Hangzhou* 310027, *China*
[3] *School of Physical Sciences, University of Chinese Academy of Sciences, Beijing* 100049, *China*
[4] *CAS Center for Excellence in Topological Quantum Computation, University of Chinese Academy of Sciences, Beijing* 100049, *China*

(Received 10 April 2019; revised manuscript received 22 May 2019; published online 9 July 2019)

Realization of a flexible and tunable coupling scheme among qubits is critical for scalable quantum information processing. Here, we design and characterize a tunable coupling element based on Josephson junction, which can be adapted to an all-to-all connected circuit architecture where multiple Xmon qubits couple to a common coplanar waveguide resonator. The coupling strength is experimentally verified to be adjustable from 0 MHz to about 40 MHz, and the qubit lifetime can still be up to 12 μs in the presence of the coupling element.

Keywords: superconducting Xmon qubit, qubit–resonator coupling, tunable coupling

PACS: 03.67.Lx, 42.50.Ct, 85.25.Cp **DOI:** 10.1088/1674-1056/28/8/080305

1. Introduction

Practical quantum computing requires a large-scale quantum network, which may build upon millions of qubits.[1,2] For this particular reason superconducting qubits, whose high scalability is guaranteed with modern microfabrication technologies, have become a promising platform and have recently attracted significant research attention.[3] A lot of work has been done to improve the qubit design and quality in a planar architecture.[4–8] The energy lifetime, which is one of the most important performance metrics for the qubit, is improved to 10 μs–50 μs for two-dimensional (2D) transmon qubits.[9,10] Various types of superconducting quantum processors, on which multiple transmon qubits are integrated with either only neighbor couplings for a 2D grid[11,12] or all-to-all couplings through a common bus resonator,[13,14] have been fabricated and successfully used for the quantum error correction, entanglement generation, and quantum simulation experiments.[12–14]

However, most of qubit-qubit and qubit–resonator coupling schemes used in these quantum processors are capacitive through non-tunable capacitors; therefore, couplings can hardly be turned off unless the qubits are detuned far away in frequency, which is difficult to implement due to limited frequency tunability. Since residue couplings may cause unwanted operation errors when qubits are supposed to be isolated in the gate control sequences, a tunable coupling scheme with a high ON/OFF coupling ratio that is also easy to operate is highly desired. In 2014, Chen *et al.*[15] reported a tunable coupler between two inductance-shunted Xmon qubits, also called Gmons. Since then, more theoretical investigations on tunable couplers have appeared.[16,17] Recently, Neill *et al.*[18] reported a blueprint for demonstrating quantum supremacy with a chain of Gmon qubits featuring neighboring tunable couplings, where they randomly turned on and off the couplings between randomly chosen Gmon qubits to allow quantum excitations to shuttle among the qubit chains. Since the couplers are the only elements being actively controlled during the experimental sequences, the coupler performance really determines whether or not the quantum supremacy experiment with Gmon qubits will succeed.

In this article, we show a variant of the Gmon coupling scheme that can be adapted to an all-to-all connected circuit architecture, an inductive coupler used between an Xmon qubit and a coplanar waveguide resonator. By changing the flux in the Josephson-junction loop of the coupler, the qubit–resonator coupling can be turned on and off at will. The coupling strength is experimentally verified to be adjustable from 0 MHz to about 40 MHz, and the energy relaxation time of the Xmon qubit can still be up to 12 μs with the coupler in use.

*Project supported by the National Key Research and Development Program of China (Grant Nos. 2017YFA0304300 and 2016YFA0300600), the National Natural Science Foundation of China (Grant Nos. 11725419 and 11434008), and the Strategic Priority Research Program of Chinese Academy of Sciences (Grant No. XDB28000000).

†Corresponding author. E-mail: hhwang@zju.edu.cn
‡Corresponding author. E-mail: dzheng@iphy.ac.cn

© 2019 Chinese Physical Society and IOP Publishing Ltd

2. Design and fabrication

As shown in Fig. 1(a), to enable the inductive coupling element, the traditional Xmon qubit is shunted with an additional line inductance, L_g. The inductance line (orange color) goes across the bus resonator via an airbridge and, together with the resonator's center trace, divides the ground into four quadrants. The first and third quadrant host a gradiometer loop with a Josephson junction at the input as the tunable coupler, which is almost insensitive to the external perturbing flux noise.

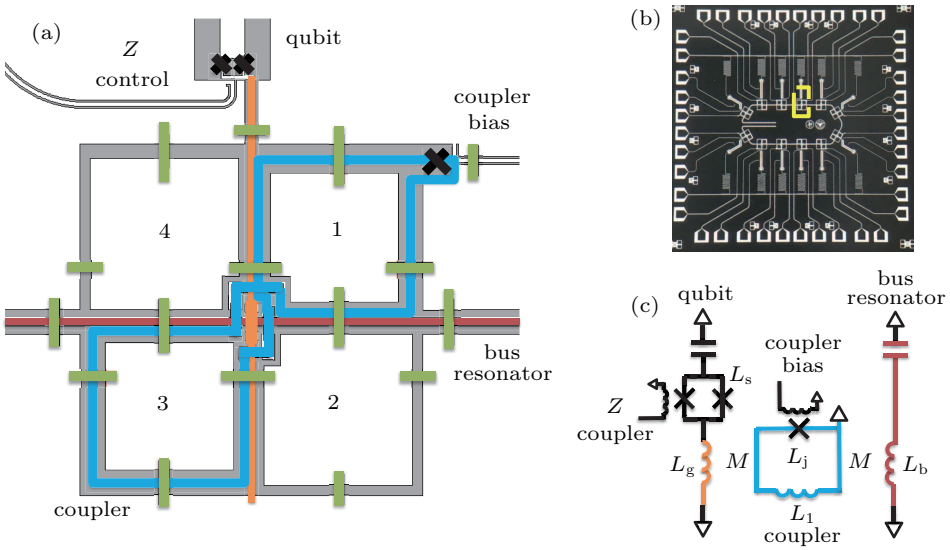


Fig. 1. (a) Layout schematic diagram of tunable coupler. (b) Optical micrograph of entire circuit chip featuring multiple Xmon qubits coupled to central bus resonator. Schematic in panel (a) refers to area enclosed in yellow square. (c) Equivalent circuit schematic plot showing Xmon qubit, bus resonator, and tunable coupler in between. Cross symbol refers to Josephson junction.

The Xmon qubit consists of a line-shaped capacitor resonating with a nonlinear inductor $L_s = 8.1$ nH from a dc SQUID. To minimize the interference of the shunting inductance, we use a linear inductor $L_g = 0.31$ nH so that $L_g \ll L_s$. When current I flows through the qubit, the magnetic flux Φ that can be sensed by the bus resonator via the coupler is

$$\Phi = \frac{M^2}{\mathrm{i}\omega L_c}\frac{\mathrm{d}I(t)}{\mathrm{d}t}, \tag{1}$$

where ω is the frequency of the oscillating current, $M = 0.085$ nH is the qubit–coupler mutual inductance, and it is also the coupler–resonator mutual inductance, and $L_c = L_l + L_j/\cos\varphi_j$ is the total inductance of the coupler. Here $L_l = 0.81$ nH is the geometric loop inductance, $L_j = 0.9$ nH is the Josephson junction inductance, and φ_j is the phase difference across the junction. With the screening parameter $\beta = L_l/L_j < 1$ for this rf-SQUID, no hysteresis in flux will affect the tuning.

The effective mutual inductance M' between the Xmon qubit and the bus resonator can be calculated from

$$M' = \frac{\Phi}{I} = \frac{M^2}{L_c}. \tag{2}$$

Therefore, the effective coupling strength g between the qubit and bus resonator is

$$g = \frac{1}{2}\frac{\sqrt{\omega_q\omega_b}}{\sqrt{L_qL_b}}M' = \frac{1}{2}\frac{\sqrt{\omega_q\omega_b}}{\sqrt{L_qL_b}}\frac{M^2}{L_c}, \tag{3}$$

where $L_q = L_g + L_s/\cos\varphi_s$ is the qubit inductance, φ_s is the phase difference across the SQUID, $L_b = 1.13$ nH is the inductance of the bus resonator, and ω_q (ω_b) is the resonant frequency of the qubit (bus resonator). When $\varphi_j = \pi/2$ for the Josephson junction in the coupler, L_c approaches to infinity so that the effective coupling strength, g, approaches to zero.

A device was fabricated with this design, as shown in Fig. 1(b). First, 100-nm-thick aluminum film was deposited on a sapphire substrate by electron beam evaporation with a base pressure better than 10^{-9} Torr (1 Torr = 1.33322×10^2 Pa). Second, a standard wet-etch process was used to define the overall wirings of the circuit: Photoresist (SPR955) was spin coated and then the structures, other than the Josephson junctions or airbridges, were defined on the coated photoresist by photolithography, following which the etchant was used to transfer the lithography pattern onto the aluminum film. Third, two types of Josephson junctions — one is for the qubits and the other one for the couplers — were fabricated using the Dolan-bridge technique[19] with different exposure doses: 500 nm of MAA and 300 nm of PMMA that were spin coated on the top of the aluminum wirings sequentially, with AR-P 5090 as the conducting layer on the top. Subsequently, the Josephson junctions were patterned by E-beam lithography. Following which, the Ar ion cleaning and the double angle evaporation of two layers of aluminum films with an oxidation process sandwiched in between were carried out in E-beam evaporator. Finally, airbridges were fabricated in a similar way to that described in Ref. [20]. The device was then measured

in the dilution refrigerator.

3. Results and discussion

As shown in Fig. 2, we first benchmark the qubit coherence performance with an existing coupler. A typical energy relaxation time in several qubits is about 12 μs, and a typical phase relaxation is about 4 μs near the optimal bias point (which is not shown here). These results are comparable to those reported in Ref. [15]. Therefore, we conclude that the coupler, though imposing complications in the device fabrication, interferes negligibly with the qubit lifetime.

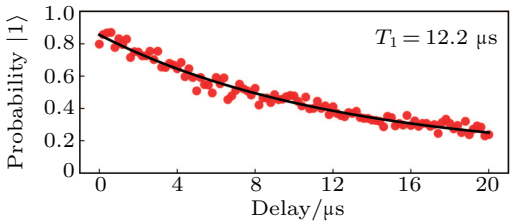


Fig. 2. Qubit $|1\rangle$-state probability *versus* delay time, showing energy relaxation process at 4.917 GHz. Line is a fit for $T_1 = 12.2$ μs.

Figure 3(a) demonstrates the functionality of the tunable coupler, where the coupling strength data (dots) are compared with the numerical calculations (line). The experimental data are processed from the measured swap dynamics between the qubit and bus resonator by using the pulse sequence shown in Fig. 3(b). With the coupler bias fixed, we first drive a π-pulse to excite the qubit at 5.63 GHz to its $|1\rangle$ state, following which we apply a square pulse with a variable amplitude of z-pulse amplitude (ZPA) to the qubit flux line, so that the qubit is tuned to a frequency around the bus resonator for energy swap dynamics with a variable delay time. The resulting qubit $|1\rangle$-state probability P_1 is measured right after the interaction, which is plotted as delay time *versus* ZPA in Fig. 3(c). The well-defined Chevron patterns indicate the energy swap process, and the period along the delay axis in the center of a Chevron pattern correlates with the coupling strength. It is seen that the coupling strength between the qubit and bus resonator varies with the coupler bias, which is in agreement with Eq. (3). The coupling strength increases quickly as the coupler bias is tuned close to half the flux quanta, and the experimentally measured coupling strength can be up to −42.7 MHz. We note that the negative sign here is due to the fact that φ_j of the coupler junction takes a value near π for $L_c = L_l + L_j/\cos\varphi_j$ in Eq. (3), while Fourier transform of the P_1 data in Fig. 3(c) only gives the amplitude of the coupling strength. The experimentally characterized range of the coupling strength is from 0 to about 40 MHz.

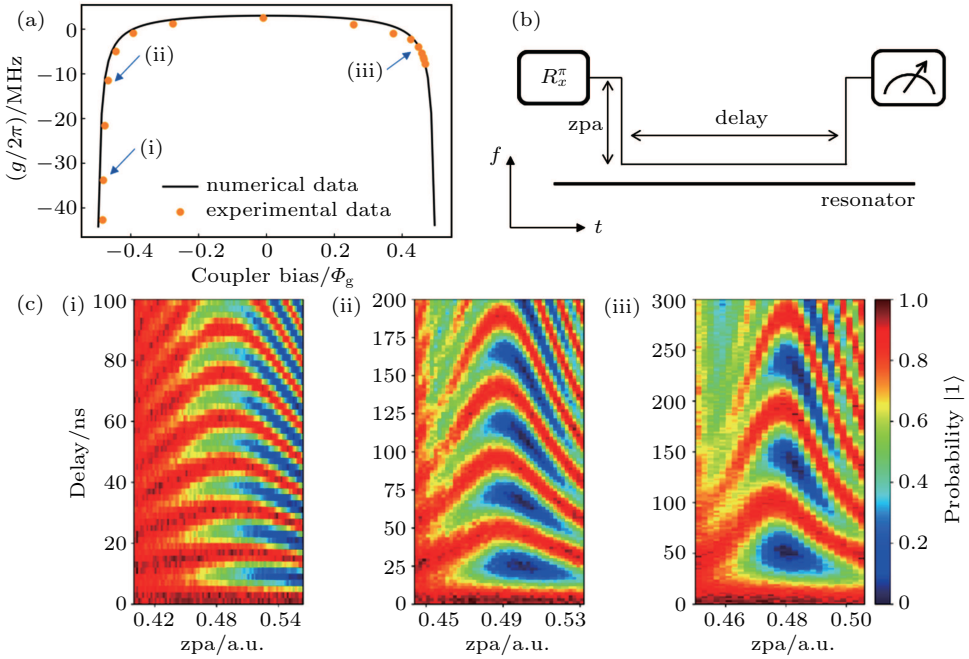


Fig. 3. (a) Measured coupling strength, $g/2\pi$ *versus* coupler bias (dots) in comparison with the numerical calculation (line). (b) Experimental pulse sequence used for the qubit–resonator swap dynamics, where qubit is excited to $|1\rangle$ at 5.63 GHz and then biased with ZPA to a fixed frequency around the resonator for energy exchange process. (c) Qubit $|1\rangle$ state probability, P_1 (color bar on the far right) and delay time *versus* qubit's ZPA, measured with the experimental pulse sequence shown in panel (b) at three coupler biases as numbered in panel (a). The coupling strength is estimated from Fourier transform of the data in panel (c) (For clarity in display the y scales are different for the color plots).

4. Conclusions and perspectives

We have designed and fabricated a tunable coupler between an Xmon qubit and a coplanar waveguide resonator. With the qubit–resonator swap dynamics, we experimentally show that the coupling strength can be adjusted from 0 MHz to about 40 MHz, and the qubit energy relaxation time can still be up to 12 μs. This tunable coupler design can be easily adapted to an all-to-all connected circuit architecture where multiple

qubits couple to a common bus resonator, and therefore will become an active building block to minimize the crosstalk error for scalable quantum electronics.

Acknowledgment

The authors thank Fengliang Dong, Peipei Chen form the National Center for Nanoscience and Technology and Haifang Yang, Aizi Jin, Guangzhou Geng, and Shi Yan from Laboratory of Microfabrication, Institute of Physics, Chinese Academy of Sciences for help in the micro-fabrication of samples.

References

[1] You J Q and Nori F 2007 *Physics Today* **58** 42
[2] Nielsen M A and Chuang I 2011 *Quantum Computation Quantum Information*, **10**th edn. (Cambridge: Cambridge University Press) p. 47
[3] Devoret M H and Schoelkopf R J 2013 *Science* **339** 1169
[4] Nakamura Y, Pashkin Y A and Tsai J S 1999 *Nature* **398** 786
[5] Chiorescu I, Nakamura Y, Harmans C and Mooij J E 2003 *Science* **299** 1869
[6] Koch J, Yu T M, Gambetta J, Houck A A, Schuster D I, Majer J, Blais A, Devoret M H, Girvin S M and Schoelkopf R J 2007 *Phys. Rev. A* **76** 042319
[7] Manucharyan V E, Koch J, Glazman L I and Devoret M H 2009 *Science* **326** 113
[8] Barends R, Kelly J, Megrant A, Sank D, Jeffrey E, Chen Y, Yin Y, Chiaro B, Mutus J, Neill C, O'Malley P, Roushan P, Wenner J, White T C, Clel, A N and Martinis J M 2013 *Phys. Rev. Lett.* **111** 080502
[9] Wang H, Hofheinz M, Wenner J, Ansmann M, Bialczak R C, Lenander M, Lucero E, Neeley M, O'Connell A D, Sank D, Weides M, Cleland A N and Martinis J M 2009 *Appl. Phys. Lett.* **95** 233508
[10] Gambetta J M, Murray C E, Fung Y K K, McClure D T, Dial O, Shanks W, Sleight J W and Steffen M 2017 *IEEE Trans. Appl. Supercond.* **27** 1
[11] Barends R, Kelly J, Megrant A, *et al.* 2014 *Nature* **508** 500
[12] Kelly J, Barends R, Fowler A G, *et al.* 2015 *Nature* **519** 66
[13] Song C, Xu K, Liu W, Yang C, Zheng S B, Deng H, Xie Q, Huang K, Guo Q, Zhang L, Zhang P, Xu D, Zheng D, Zhu X, Wang H, Chen Y A, Lu C Y, Han S and Pan J W 2017 *Phys. Rev. Lett.* **119** 180511
[14] Xu K, Chen J J, Zeng Y, Zhang Y R, Song C, Liu W, Guo Q, Zhang P, Xu D, Deng H, Huang K, Wang H, Zhu X, Zheng D and Fan H 2018 *Phys. Rev. Lett.* **120** 050507
[15] Chen Y, Neill C, Roushan P, *et al.* 2014 *Phys. Rev. Lett.* **113** 220502
[16] Geller M R, Donate E, Chen Y, Neill C, Roushan P and Martinis J M 2014 arXiv: 1405.1915[cond-mat,physics:quant-ph]
[17] Yan F, Krantz P, Sung Y, Kjaergaard M, Campbell D L, Orlando T P, Gustavsson S and Oliver W D 2018 *Phys. Rev. Appl.* **10** 054062
[18] Neill C, Roushan P, Kechedzhi K, *et al.* 2018 *Science* **360** 195
[19] Dolan G J 1977 *Appl. Phys. Lett.* **31** 337
[20] Chen Z, Megrant A, Kelly J, Barends R, Bochmann J, Chen Y, Chiaro B, Dunsworth A, Jeffrey E, Mutus J, O'Malley P, Neill C, Roushan P, Sank D, Vainsencher A, Wenner J, White T, Clel A and Martinis J 2014 *Appl. Phys. Lett.* **104** 052602